E-Journal of Advanced Maintenance Vol.1 (2009) 68-76
Japan Society of Maintenology

Investigations of Multi-frequency Algorithms for Detection of Defects in FBR Magnetic Steam Generators Tubes Covered with Sodium

Ovidiu MIHALACHE,* Shinya MIYAHARA, Toshihiko YAMAGUCHI, Takuya YAMASHITA
[1] *Japan Atomic Energy Agency, Fast Breeder Reactor Plant Engineering Research Center, 1 Shiraki, Tsuruga-shi, Fukui-ken, 919-1279, Japan*

(Received; January 20th, 2009)

Abstract. In the present paper it is presented the performance of multi-frequency eddy currents algorithms to cope with the eddy current signal from both sodium structures located on the outer surface of magnetic steam generator tubes surface as well as support plates of steam generator tubes. The algorithm improves the signal to noise ratio of defects detection even when these are located under steam generator support plates. Experimental measurements of defects signals using eddy currents, when there is or there is no sodium on the outer tube surface, are used to validate reliable computer simulation models in order to investigate and optimize the multi-frequency algorithms. The parameters of the most reliable multi-frequency algorithm, based on two or three excitation frequencies and using both simulated and experimental remote field eddy current signals, are found out for both cases when sodium adhere or not to the SG tube surface and a defect is placed or not under sodium bands or SG supports plates.

KEYWORDS: steam generator, fast breeder reactor, multi-frequency, remote field eddy current, sodium, support Plate, finite element method

1. Introduction

In the magnetic heat exchanger tubes of Fast Breeder Reactors (FBRs) liquid sodium is used as an intermediate heat-transfer fluid. A high pressure water flows inside of tubes while a low pressure sodium flows runs inside the vessel containing the steam generator (SG) tubes. Due to the high chemical reactivity of sodium with water, penetration of SG tubes wall has to be avoided by all means, and therefore earlier defect detection before wall penetration during the in-service inspection (ISI) is required to increase the safety of SG tube components.

Remote Field Eddy Current Technique (RF-ECT) is a special method able to detect with equal sensitivity both inner and outer defects in ferromagnetic SG tubes [1-2]. The RF-ECT inspection system includes both an electromagnetic excitation device and a detection coil that measures the electromagnetic disturbance due to a defect in a tube. ISI is performed at room temperature after sodium from SG vessel was drained and cooled down from several hundreds degrees to room temperature. After draining, sodium adheres to the outer tube surface in a thin layer. In a previous work it was estimated that sodium thickness layer was between 10 and 50 μm using comparison between eddy current measurements and accurate finite element simulations [3, 4]. Because solid sodium is also highly electrical conductive, but with a relative magnetic permeability close to one, its presence on the outer tube surface affects the electromagnetic disturbance signal from existing cracks located on the outer tube surface. When ECT inspection analysis is conducted from inside of the SG tubes, due to the inability to access the outer SG tube surface, the noise in the signal due to irregularities in sodium layer thickness or sodium drops or bands near SG support plates can mask the signal from a defect, making difficult to interpret the results in real ISI conditions. Previously numerical simulations, for both magnetic and non-magnetic SG tubes, showed that by using a

*Corresponding author, E-mail: Ovidiu Mihalache, mihalache.ovidiu@jaea.go.jp

ISSN – 1883 – 9894/09

multi-frequency ECT algorithm approach it is possible to eliminate the uncertainties from sodium signal even when there is a possibility that sodium drops or bands appear next to support plates (SP) [5-6]. However, the reliability of numerical simulations could be confirmed only with experimental measurements in the absence of sodium, raising the question of whether or not the algorithm changes or could be trusted in the presence of sodium layer and what is its performance using experimental data.

The multi-frequency techniques is a well-known method which was previously applied in the signal processing of eddy current signal from tubes and pipes in nuclear power plants. Earlier work shown in [7-9], proved the feasibility of the method but only for water cooled reactors and using non-ferromagnetic SG tubes and bobbin type coils excited by classical eddy current probes.

In the present paper, the authors investigates the feasibility of multi-frequency remote field eddy current algorithms to suppress SG support plates influences in the presence of unknown sodium layer thickness and sodium structures located nearby. Optimized multi-frequency algorithms are investigated using first numerical finite element simulations, calibrated with experimental measurements, in order to enhance the detection of outer tubes defects for various sodium layer thicknesses. The parameters of the multi-frequency algorithm are determined in the case when sodium adheres or not to the outer SG tube surface using numerical finite element simulations. The multi-frequency algorithms are checked and verified using directly experimental measurements from defects under SP when these are covered by thin sodium layer.

The paper is organized in the following way. First, an experimental set-up is described to investigate the eddy current effect due to sodium structures located on the outer surface of magnetic SG tubes. Next, eddy current (EC) finite element (FE) simulations are used to model the sodium effect and to evaluate the maximum noise arising from sodium structures and SP covered by sodium. Simulations are validated with experimental measurements form defects and SP when there is or not sodium on the outer SG tube surface. Suppression of SP and sodium signal is investigated using accurate numerical multi-frequency algorithms to evaluate the most optimized method and then the algorithms are applied directly to experimental data to increase detection of defects even when these are located under SG support plates.

2. Experimental Set-Up to Investigate Sodium Effect on the ECT Signals

An experiment was set-up to investigate what is the eddy current effect of small layers of sodium adhering to steam generator tubes. Two SG tubes, one made of austenitic stainless steel and the other being ferromagnetic, were introduced in a cylindrical tank, as it is shown in Fig. 1. Several SPs were attached to the tubes in both upper and lower part. In the tube were machined two outer grooves (OD) 20% from the tube wall thickness (tw), 10 mm wide and one of the support plates was located just above one defect. A view of the OD in the helical part of the SG tubes is shown in Fig. 2a. Liquid sodium at 200^0 C was first introduced in the tank and then its temperature was quickly raised to 500^0 C. Sodium was kept in the tank at high temperature for two hours and then its temperature was again decreased to 200^0 C. At this point, sodium was drained and the tank was cooled down in one day to the room temperature. The RF-ECT signals from the magnetic SG tubes, as well as from the support plates were recorded both before sodium was introduced in the tank and after sodium was drained and the tank temperature was around 30^0 C. A fiberscope camera was introduced in the tank in order to visualize the sodium deposits and sodium adherence to the magnetic SG tubes as well to the SP.

Fig. 2b shows the sodium deposits near the outer groove. The defect, as well as the tube are covered by a thin sodium layer with a variable layer thickness. Fig. 2c shows a view of a sodium drop on SG tube formed after sodium draining. An estimation of the raw-image from fiber-scope camera evaluated this drop to 4-5 mm height and 6-8 mm diameter.

Fig. 3 shows a view of the straight SP (support plate located on the straight part of SG tube) before and after sodium adherence. An outer groove 20%tw, 10 mm wide, not visible in the pictures is located under SP. Images taken with the fiberscope shows that sodium adheres to the SP and also sodium enters in the space gap between SP and SG tube. However it is difficult to quantitatively estimate how much sodium fills this gap and if sodium fills or not the defect under SP.

Fig. 1. View of the steam generator tubes and support plates inside of sodium tank

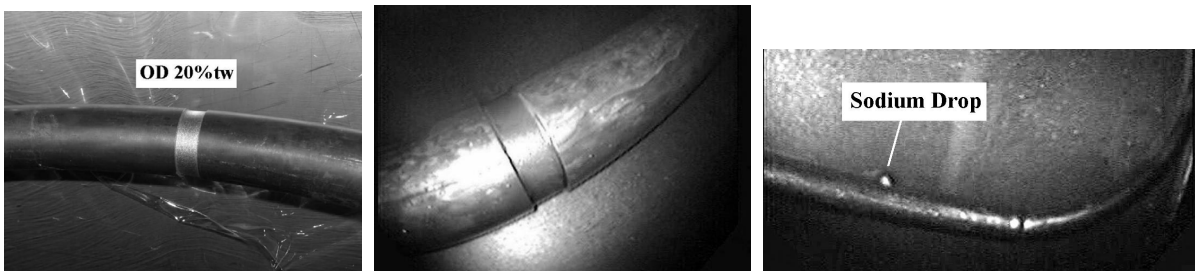

a) b) c)

Fig. 2. a) Groove 20%tw, 10 mm wide, on helical part of SG tube;
b) Sodium structures around defect; c) Visualization of a sodium drop located on the top of SG tube

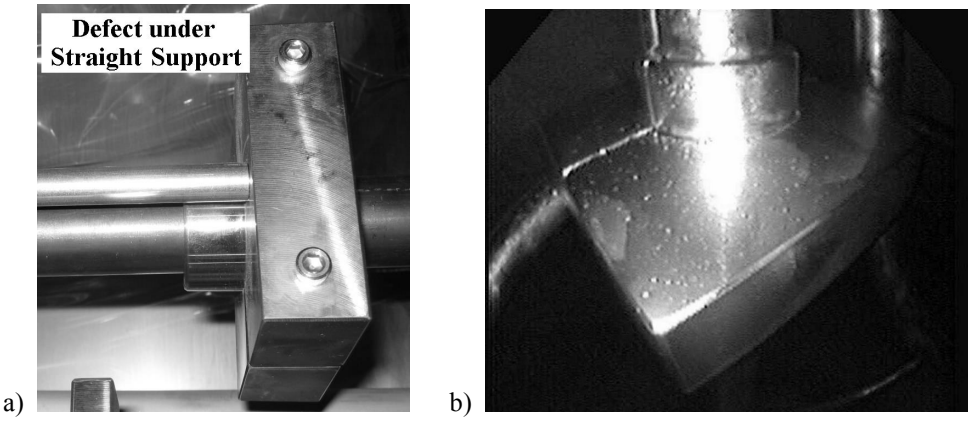

a) b)

Fig. 3. a) Configuration of straight support plate (groove 20%tw 10 mm is located under SP); b) Adherence of sodium to the straight SP

3. Finite Element Simulation for Sodium and Steam Generator Support Plate RF-ECT Signal

Numerical simulations were conducted using a finite element code [4] which can model the electromagnetic interaction between electromagnetic field produced by the RF-ECT coils system and ferromagnetic SG tube and calculate the electromagnetic disturbance due to a defect in the tube. The RF-ECT probe consists in two excitation systems, far from each other with a differential detections system, based on the bobbin coil type, located between the two excitation devices. The current is flowing in the same direction in both excitation coils.

The presence of sodium layer on the outer tube surface modifies the electromagnetic path signal during eddy current measurements due to the sodium high electrical conductivity (23.8×10^6 S/m). In a previous paper [3], the authors found out, by matching numerical remote field ECT simulations with experimental measurements, that the medium thickness of the sodium layer deposit on the outer SG tube surface is less than 50 μm. However, the true thickness of the sodium layer cannot be known in advance, as could be seen in the pictures taken with the fiberscope during experiment.

In numerical analysis, sodium layer thickness was set to be between 0.01 and 0.1 mm in order to evaluate the maximum noise which could came from the sodium layer. The geometrical model of the SP covered by sodium and located on the straight part of SG tubes, of sodium bands covering outer SG defects and sodium bands located next to SP is presented in Fig. 4. Sodium can fills completely or partially the defect as it is located under SP.

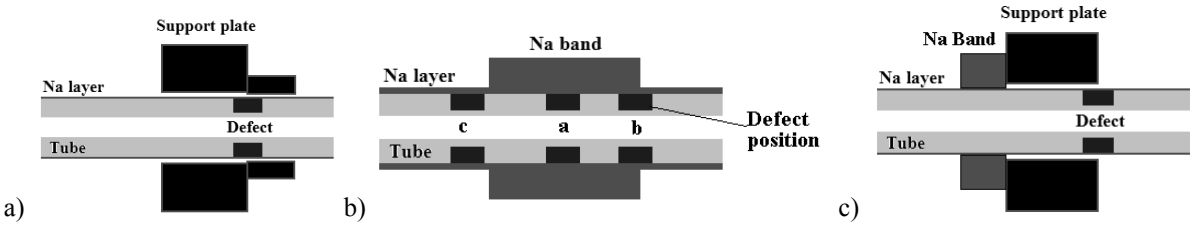

Fig. 4. Geometrical model for: a) straight SP covered by a thin sodium layer; b) defect under sodium band; c) sodium structures near SP

A numerical evaluation of the RF-ECT signal of sodium layer and sodium band effect is illustrated in Fig. 5 . As sodium layer thickness increases the outer defect ECT signal decreases. Also, the sodium band signal is similar with the defect signal. During numerical simulations were investigated several sizes (height up to 5 mm, up to 40 mm wide) of sodium bands in order to cover a wider range of problems. The variation of signal coming only from sodium bands is shown in Fig. 5b.

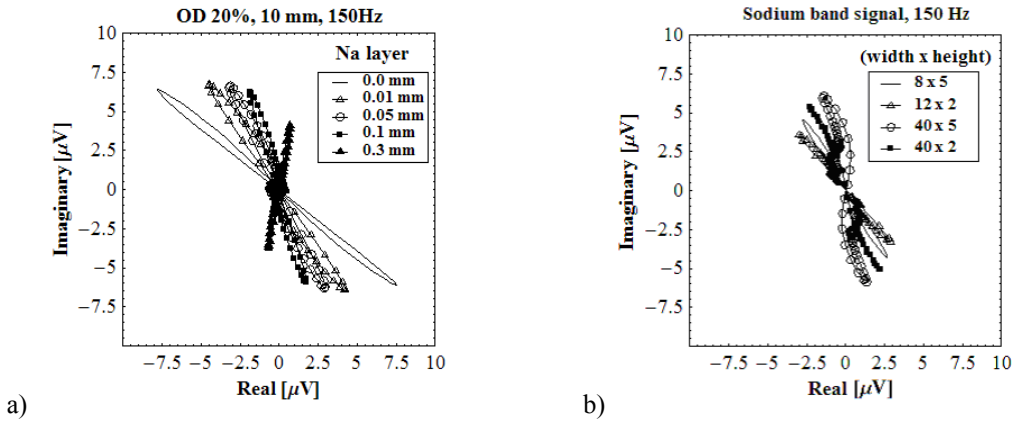

Fig. 5. Simulation of RF-ECT signal from: a) OD20%tw, 10mm partially filled with sodium; b) a sodium band with different sizes

Numerical simulations were validated with experimental measurements of outer groove signal in both cases when sodium adhere or not to the outer SG tube surface (see Fig. 6). While the agreement between simulation and measured data was very good in the absence of sodium, a small discrepancies was observed in the presence of sodium. This is because simulations took into account only a constant sodium layer thickness. However, the results are in good agreement and confirmed that the medium sodium layer thickness size is 30 μm, which was in agreement with previous simulation results that determined a maximum 50 μm sodium layer thickness [3].

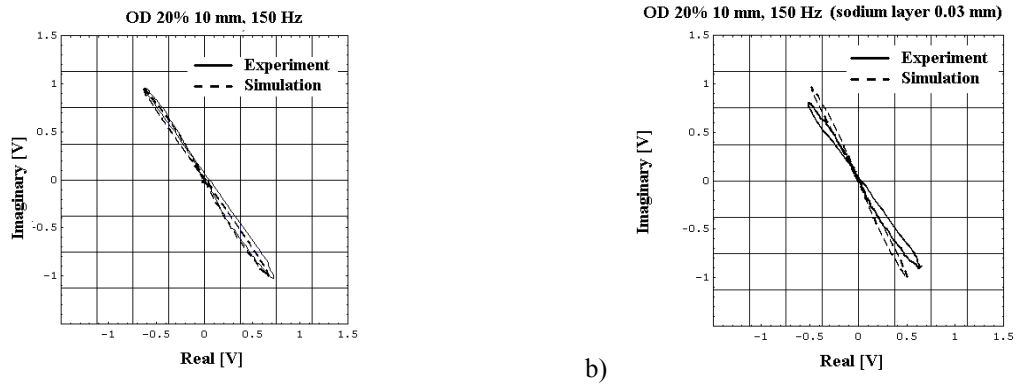

a) b)

Fig. 6. Comparison between simulations and measurements in absence of sodium layer for OD 20% tw, 10mm in a helical tube: a) without sodium; b) SG tube covered by sodium

In Fig. 7a it is shown the comparison between numerical simulation of straight SP and measured data when there is no sodium on the outer SG surface. In Fig. 7b, a defect under SP was added in the numerical analysis. The small discrepancies between simulation and measured data in Fig. 7b could be due to the unknown gap between SP and defect, because the SPs simulated in Fig. 7a and Fig 8a are two different SPs located on different part of the tube, one SP with a defect under it and the other one without any defect.

Fig. 8 shows the same simulations like in Fig. 7 but in the presence of sodium. A very good agreement was obtained, despite the complexity of the real model, confirming the validity of the numerical electromagnetic model for all parts involved in the analysis: magnetic SG tubes, SP, unknown distribution of sodium layer. However, in the visual inspection of the experiment could not be seen any large sodium structure formation near SP. But this does not rule out that a sodium structure could not be formed near SP and consequently this situation was taken into consideration in numerical simulations.

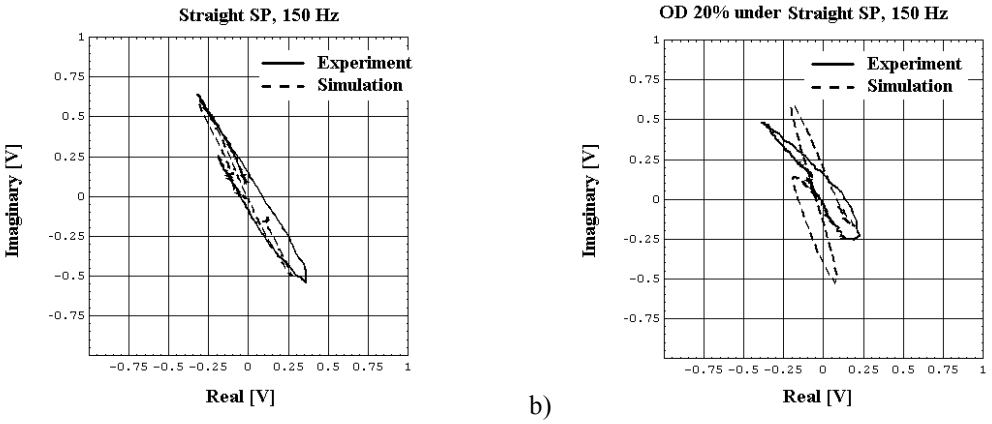

a) b)

Fig. 7. Comparison between simulations and measurements in absence of sodium layer for : a) straight SP; b) OD 20%tw under straight SP

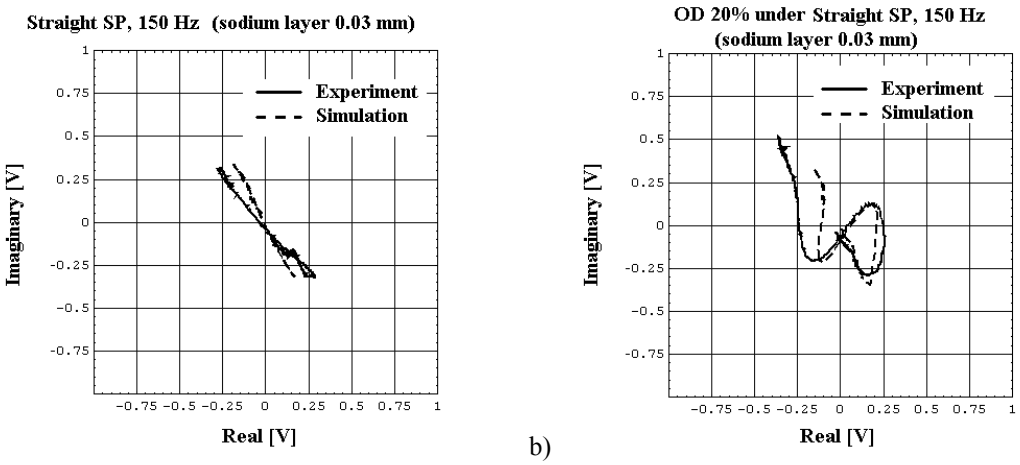

a) b)

Fig. 8. Comparison between simulations and measurements in the presence of sodium: a) straight SP; b) OD 20%tw under straight SP

4. Multi-Frequency Algorithm to Suppress Both SG Support Plate and Sodium Signal

The multi-frequency algorithm is based on the assumption that by combining the RF-ECT signal at several frequencies (low and high frequencies), the signal from sodium structures and support plates can be reduced while the signal from existing covered defects is enhanced. The algorithm can be successful only in the case when sodium bands signal and defect signal have a different pattern variation with frequencies. In the particular case of the studied RF-ECT probe and SG tube parameters the authors found through numerical simulations that this assumption remains valid.

Let's suppose we have the RF-ECT defect signal S_i at several frequencies ν_i. Then, the "j" multi-frequency algorithm compute the mix signal S^j by combining the S_i signals using the linear parameter α_i as in Eq. 1, where Q_i is the linear operator defined by Eq. 2.

$$S^j = \sum_{i=1}^{n} \alpha_i \cdot Q_i[S^j{}_i(\nu_i)] \tag{1}$$

$$Q_i = \begin{pmatrix} \cos\theta_i & -\sin\theta_i \\ \sin\theta_i & \cos\theta_i \end{pmatrix} \tag{2}$$

The "k" noise in the signal (in our case SP and sodium signal) can be written in a similar way (see Eq. 3), where "k" represents different sources of noise as: sodium layer, sodium drop, support plate and others.

$$N^k = \sum_{i=1}^{n} \alpha_i \cdot Q_i[N^k{}_i(\nu_i)] \tag{3}$$

$$\begin{cases} \min\left\|N^k\right\| \\ \max\left(\dfrac{\left\|S^j\right\|}{\left\|N^k\right\|}\right) \end{cases} \tag{4}$$

The optimum parameters of the multi-frequency algorithms , (α_i, θ_i) are found out by minimizing the norm of all known noise and maximizing the signal/noise ratio as is shown in Eq. 4.

Using numerical simulations of the defect signal and sodium layer and bands signals the parameters of the multi-frequency algorithm are calculated in that way to reduce the sodium bands signal. These parameters are determined in the case of "sodium approximation" (there is sodium layer outside of SG tube). The reason of doing this approximation is that the sodium signal will be considered as an additional noise source, since it is not possible to have knowledge of the sodium layer thickness or size of the sodium drops or bands.

In numerical simulations were investigated all frequencies from 50 to 500 Hz in a 50 Hz step. The best mixing frequencies were found to be in the range 100-200 Hz for this particular ECT sensor and SG tube parameters. For other sensors or SG tube geometries, numerical simulations confirmed that parameter of the multi-frequency algorithm modifies as well. A numerical analysis has to be conducted for every specific ECT sensor configuration to find out the optimum working parameters. An example of the algorithm is illustrated in Fig. 9 using numerical simulations. The signal from a defect in several position (see Fig.4b) under a sodium band is enhanced while the sodium band an layer signal is reduced to a central spot.

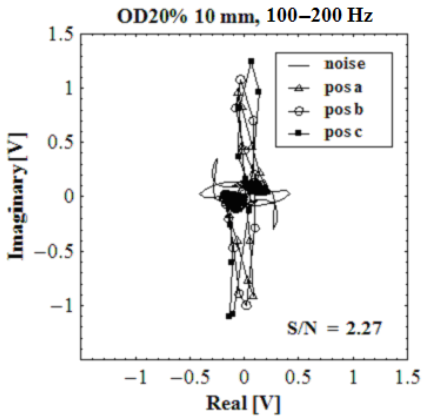

Fig. 9. Simulation of multi-frequency analysis to suppress sodium band and enhance defect signal

Using numerical simulations it was found out that for ferromagnetic SG tubes it is not possible to extrapolate the same multi-frequency algorithm to the suppression of the steam generator supports plates and a different multi-frequency tuned algorithm it is required.

In Fig. 10 it is presented the application of multi-frequency algorithm to the "no sodium" condition – there is no sodium on the outer SG tube surface. Fig. 10a is the result obtained using numerical simulations while the signal in Fig. 10b-c is the result obtained using measured data. Figures 10a-c show the best results among all combined multi-frequency algorithms, using the following frequency combinations: (150Hz-450Hz), (150Hz-600Hz), (450hz-600Hz) and (150Hz-450Hz-600Hz)). The 2-frequency mix combination (450Hz-600Hz) showed the best signal/noise ration in suppressing the SP signal in the absence of sodium. The signal from an outer defect under straight SP of magnetic SG tube is enhanced. The algorithm can cope well with the noise in the experimental data and only a three-frequency algorithm (shown in Fig. 10c) increased the signal/noise ratio.

In Fig. 11 it is shown the result of application of multi-frequency algorithm when there is sodium on the outer SG tube surface and the defect is located under SP. Despite there is no knowledge about how sodium fills the gap between SP and tube and if the defect is filled completely or partially with sodium, the algorithm can enhance the defect signal and suppress SP and sodium signal. The parameters of the multi-frequency algorithm changes as a thin sodium layer adheres to the outer SG tube surface. It was found that in this case a (150Hz-450Hz) algorithm can cope better with the noise from sodium (Fig 11b).

By validating numerical simulations with measured data, in the presence of sodium, the new multi-frequency algorithm parameters are determined and a three-frequency algorithm is shown in Fig 11c to give also an enhanced signal/noise ratio compared to the two-frequency algorithm approach.

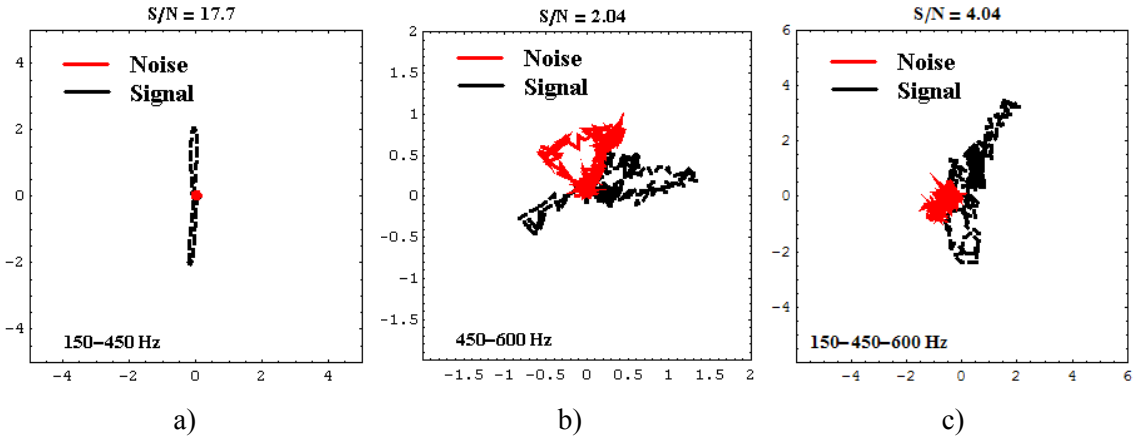

Fig. 10. Application of multi-frequency algorithm in the absence of sodium to suppress support plate signal and enhance defect signal to: a) simulated data; b) experimental data (two-frequencies algorithm); c) experimental data (three-frequencies algorithm)

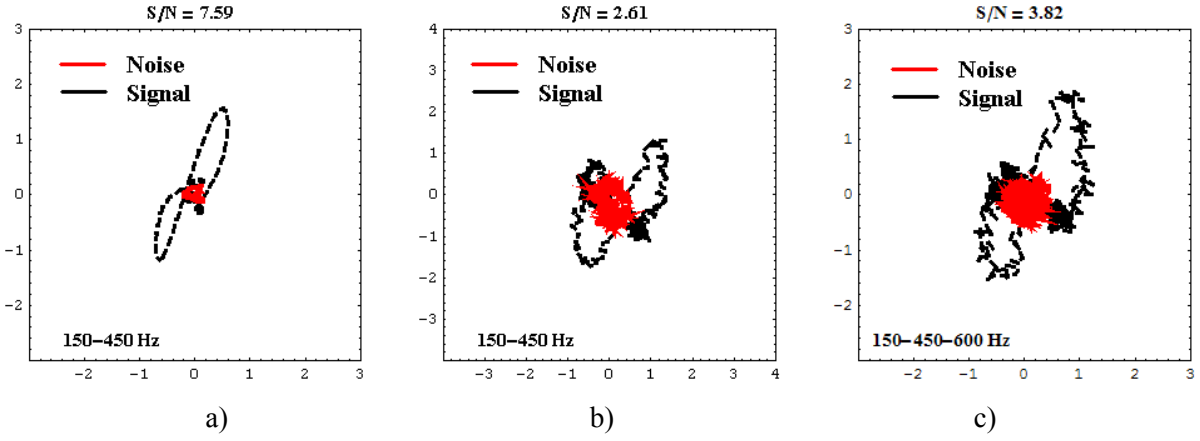

Fig. 11. Application of multi-frequency algorithm in the presence of sodium to suppress support plate and sodium signal and enhance defect signal to: a) simulated data; b) experimental data (two-frequencies algorithm); c) experimental data (three-frequencies algorithm)

Through numerical simulations it was studied how the sodium layer affects the ECT signal. By validating numerical simulations with measured data, the performances of linear multi-frequency algorithm was investigated to suppress both sodium and SP signal in order to reveal defects under SP of magnetic SG tubes.

5. Conclusion

In the paper were presented validations of RF-ECT signal from defects under support plates of magnetic steam generator tubes with experimental measurements in both cases when sodium adheres or not to the outer SG tube surface. Multi-frequency RF-ECT algorithms were calibrated with numerical simulation in order to optimize the parameters of multi-frequency algorithms and then applied directly to experimentally measured data. Detection of outer groove under the straight SP of magnetic SG tubes could be enhanced in both cases where there is or there is no sodium on the outer surface of SG tubes. A three-frequency algorithm, validated with experimental data, was able to better suppress both SP and sodium signal and reveal a hidden defect under the straight SP. The optimized parameters change as the analysis moves from the no sodium to sodium approach.

References

[1] ***, Nondestructive Testing Handbook (2nd edition), 4, Electromagnetic Testing, 1986.
[2] D. L. Atherton, S. Sullivan and M. Daly, A remote field eddy current tool for inspecting nuclear reactor pressure tubes, Br. J. Nondestructive Testing 30, 1988, pp 22-28.
[3] O. Mihalache, K. Yokoyama, M. Ueda and T. Yamashita, Evaluation of the effect of sodium in steam generator tubes using remote field, Studies in Applied Electromagnetics and Mechanics, 24, 2004, pp.223-230.
[4] O. Mihalache, Advanced remote field computational analysis of steam generators tubes, IOS Press, Electromagnetic Nondestructive Evaluation VII, Studies in Applied Electromagnetics and Mechanics 26, 2006, pp 220-227.
[5] O. Mihalache, T. Yamaguchi, M. Ueda and T. Yamashita, Analysis of defect detection in steam generator tubes of FBR under support plates and in the presence of sodium using multi-frequency eddy currents algorithm, The 15th International Conference on Nuclear Engineering, Nagoya, Japan, April 22-26, 2007.
[6] O. Mihalache, T. Yamaguchi and T. Yamashita, Numerical simulations of a multi-frequency eddy current algorithm for improved defect detection in magnetic SG tubes covered by sodium in FBRs, The 4th Conference of Japan Society of Maintenology, Fukui, Japan, July 2-3, 2007, pp. 59-62.
[7] S. Kumano, N. Kawase, K. Kawata and A. Kurokawa, Signal processing of rotating pancake eddy current signal for steam generator tubes, Proceedings of the 13th International Conference on NDE in the Nuclear and Pressure Vessel Industries, Kyoto, Japan, 22-25 May, 1995, pp. 413-420.
[8] V. Ganugapati, K. Arunchalam, P. Ramuhalli, L.Udpa and S.Udpa, A polynomial mixing algorithm for suppressing TSP signals in bobbin coil eddy current data, Electromagnetic Nondestructive Evaluation (VII), Studies in Applied Electromagnetics and Mechanics 26, IOS Press, 2006, pp. 213-219.
[9] Zhenmao Chen, Naoki Chigusa, Hiromu Isaka and Kenzo Miya, Data Processing of Corrosion Noise Polluted ECT Signals for Heat Exchanger Tubes of Cu-Ni Alloy, Electromagnetic Nondestructive Evaluation (VIII), Studies in Applied Electromagnetics and Mechanics, 24, IOS Press, 2004, pp 128-135.